



Research paper

Slope stability analysis of post-mining dumps with the use of photogrammetric geometry measurements – a case study

Magdalena Wróblewska¹, Magdalena Kowalska²,
Marian Łupieżowiec³

Abstract: Post-mining dumps are a common sight in the industrial areas of Silesia (Poland). Despite several reclamation projects, many of them still constitute an unresolved problem. It is not only a matter of unaesthetic view – they often pose a threat to the environment and the people living nearby. Despite revitalization, some dumps are not properly maintained and are at the risk of slope failure. Such places require constant geodetic observation and stability control. In this article, the example of a dump located in the city of Gliwice was used to show the possibilities offered by the use of photogrammetry and unmanned aerial vehicles (UAV) for cyclic checks of the embankment condition. The current state of the dump and the results of interventions after two incidents of slope failure, were observed. The main slopes of the terrain surface and at the selected cross-sections were determined in two flight missions. The obtained geometrical data were used in the further numerical analysis. Finite Element Method model representing one of the escarpment cross-sections was built to estimate the factor of safety and determine the main mechanisms responsible for the failure. Elastic-perfectly plastic Coulomb-Mohr model was used to describe the behaviour of the minestone and the ‘ $c - \tan \varphi$ reduction’ – for calculation of the stability. The problem of reliable material properties’ estimation was emphasized. The analysis included the impact of seepage and total head difference on the slope stability. It was concluded that the rainfall intensity had a decisive influence on the instability of the dump.

Keywords: post-mining dump, Unmanned Aerial Vehicle, photogrammetry, slope stability, seepage pressure

¹PhD., Eng., Silesian University of Technology, Faculty of Civil Engineering, Department of Geotechnics and Roads, Akademicka 5, 44-100 Gliwice, Poland, e-mail: magdalena.wroblewska@polsl.pl, ORCID: 0000-0002-4239-5026

²PhD., Eng., Silesian University of Technology, Faculty of Civil Engineering, Department of Geotechnics and Roads, Akademicka 5, 44-100 Gliwice, Poland, e-mail: magdalena.kowalska@polsl.pl, ORCID: 0000-0001-7549-2722

³PhD., Eng., Silesian University of Technology, Faculty of Civil Engineering, Department of Geotechnics and Roads, Akademicka 5, 44-100 Gliwice, Poland, e-mail: marian.lupiezowiec@polsl.pl, ORCID: 0000-0003-4863-2333

1. Introduction

Post-mining dumps are a typical element in the landscape of Upper Silesia, Poland. They have been formed during the long history of mining industry in this region (since the XVIII century), where not only the hard coal has been extracted, but also zinc and lead ores. Many of the mines no longer exist, but their waste storage sites are still present there. Some dumps have been reclaimed and designated for investment areas [1]. The successful examples are the terrain in Katowice on which Spodek Arena is located or the Silesian Park in Chorzów. In many cases, however, these landfills are not properly maintained and even despite revitalization, may pose a threat to the people and the environment. Obviously, similar issues occur in every country with mineral resources. The main problems are related to the chemical composition of the waste materials (e.g. heavy metals, toxic leachates, self-ignition) [2] and to the slope stability [3–5] to increase the volume of the landfill the steepest possible slopes are usually designed, which increases the risk of a failure. An example of such a problematic dump is the one at Pszczyńska Street in Gliwice, where slope failures occur frequently after heavy rainfalls, resulting in the closure of a significant section of a neighbouring road to vehicular traffic. Structures like that require constant geodetic observations and regular stability controls. In case of a failure, it is sometimes not easy to determine the owner and the current users of the dump – then a legal entry to the area in order to perform classical geodetic measurements becomes difficult. Additionally, due to the often steep and high slopes, performing classical measurements may be risky to the surveyors. In such cases, remote techniques are indispensable, such as the use of an Unmanned Aerial Vehicle (UAV, colloquially: ‘a drone’). The measurement results can then be used in numerical analyses of the slope stability. Of course, there still remains the problem of how to determine the values of the geotechnical parameters to be used in the constitutive models, as the landfilled material may be extremely heterogenous.

The example of the aforementioned dump has been used in this paper to present and discuss the measurement capabilities of UAV. The obtained readings enabled simulation of the observed instability with the use the Finite Element Method (FEM) method.

2. Surveying methods used for large structures

Geodetic observations of the post-mining dumps are usually conducted with the use of classical methods, which boil down to the situational and height measurements of the characteristic points of the landfill body: along the outline of its base and at the external vertices [6]. In the case of irregular structure forms, the local bends are also surveyed. The accuracy of the geodetic measurement depends on many factors, including: the technique adopted, the accuracy of the equipment, the target lengths, the observer’s skills, the environmental conditions [7–9]. The most accurate points layout can be obtained by means of the polar method, using a classical or robotic total station [9]. In order to measure the directions and distances, this technique requires establishing a position and a reference point *in situ*. Thanks to the implementation of new technologies, the x , y , z coordinates of the characteristic points may be nowadays determined also with the use

of the Global Navigation Satellite Systems (GNSS) – e.g. with the Real-Time Kinematic measurement technique. This is one of the most often used methods, allowing obtaining data quickly, without the need of forming large surveying teams (one person is enough). On the other hand, a common problem is a signal interference or lack of vision caused e.g. by the neighbouring tall buildings, trees or dense urban development. The accuracy of the total station and GNSS results depends on the number of the points measured in field [10]. It means that a direct approach to the site is necessary, which is not always possible and safe when the large and steep-sloped post-mining dumps are considered. It becomes also very time, labour and cost-consuming in large-size structures as all the points need to be surveyed one by one.

These problems may be overcome by the use of various modern methods, like: photogrammetry (based on aerial or satellite images), the airborne laser scanning (ALS) or the radar interferometry (InSAR) [11–13]. They are gaining more and more popularity due to their effectiveness (large number of points measured in a short time) and the possibility of conducting the measurements remotely. Among the mentioned methods, the best accuracy at the relatively low cost can be achieved when photogrammetric measurements conducted with the use of Unmanned Aerial Vehicles are done [14]. The obtained digital images are then processed through an algorithm in a special software. In the post-processing stage, a dense cloud of points with their x , y , z coordinates is obtained, giving a 3D model of the measured structure, based on which the needed area and/or volume of the object can be easily determined. It is also possible to compare the measurements conducted at various times to control the possible evolution of displacements and deformations of the object.

The photogrammetric methods, including the use of UAV, have been applied in many research and commercial projects, where classical survey was too risky, e.g. for measuring very high, hard-to-reach objects, like chimneys, masts, poles [15] or for maintaining high-voltage lines [16]. The UAV surveying is extremely useful for large areas, including building sites. Such a monitoring enables a constant control of the progress of construction works, with the possibility of taking measurements without compromising the safety of the surveying engineers [17–20]. The same refers to high slopes, whose stability should be regularly verified [21–23]. The cyclic observations of displacements are a valuable source of information about the condition of the object and potential risk of forming a failure surface [1].

Taking into account, that the considered post-mining dump was difficult to access and potentially unstable, the use of photogrammetry and UAV was the best solution for the cyclic observation of its state and for any further analyses.

3. Case study

3.1. Characteristics of the structure and its failure

The considered slope is a part of the post-mining dump covering more than 8 hectares of land between Pszczyńska and Bojkowska streets in Gliwice. It is a remnant of a hard coal mine ‘KWK Gliwice’ that worked for almost 90 years and ended the exploitation in 2000. Large part of the terrain has been reclaimed as a part of the ‘New Gliwice Business and

Education Center' project, the other is still exploited as a source of building materials [24]. At the length of about 600 meters along the Pszczyńska street, the escarpment with a height of about 8 m neighbours a busy road. After almost every heavy rain the deposited material slides (Fig. 2), often covering one road lane and a bus stop, completely blocking the traffic for several hours. The largest observed zone of depletion occurred in January 2022 in the close vicinity of the industrial hall (then under construction). In June 2022 it appeared again, directly next to the openwork concrete slabs that had been put on the rebuilt slope surface after the previous failure. Mudflows occurred along the whole length of the analysed section, leaving deep gullies at regular intervals.

Macroscopically the dump consists mostly of fine soils, claystone, sandstone and black unburnt carbonaceous shale with grading ranging from clayey to boulder fractions (Fig. 1), indicating that the waste contains probably the material from the main production and enrichment processes (e.g. washery) [25]. The grains and rock fragments are angular with visible fissility and hard coal occurrence.



Fig. 1. Various fractions visible in the failure zone (P2 in Fig. 2a), photo. M. Kowalska

3.2. Photogrammetric measurement using an Unmanned Aerial Vehicle

An Unmanned Aerial Vehicle was used to conduct photogrammetric measurements over the considered area. The raids were made using a quadcopter weighing ca. 1.3 kg, equipped with a camera with an 1-inch 20 MP sensor. The flight parameters were following:

- trajectory: double grid (usually dedicated to 3D models),
- altitude: 40 m – giving the resolution of 1.1 cm/pix,

- speed: 4 m/s,
- camera angle: 80 degrees,
- lateral and longitudinal coverage of photos: 80%.

The flight missions lasted no longer than 18 minutes, during which approximately 270 photos were obtained.

The measurements were conducted twice: in January 2022 and June 2022. In both cases, the post-processing stage included alignment of the photos and matching them to the ground control points (tracked using GNSS). As the result a cloud of points with the density of 500 points/m² was generated. The obtained 3D models of slopes with two characteristic cross-sections P1 and P2, used in the further analyses, are shown in Fig. 2.



Fig. 2. 3D visualization of the research area: a) 1st measurement (01.2022),
b) 2nd measurement (06.2022)

Hypsometric maps (*digital elevation models*, DEM) were also created – they are presented in Fig. 3. The resolution in the DEMs was equal to 4.3 cm/pix. The models were used to determine the detailed topography of the terrain by means of the contour lines at

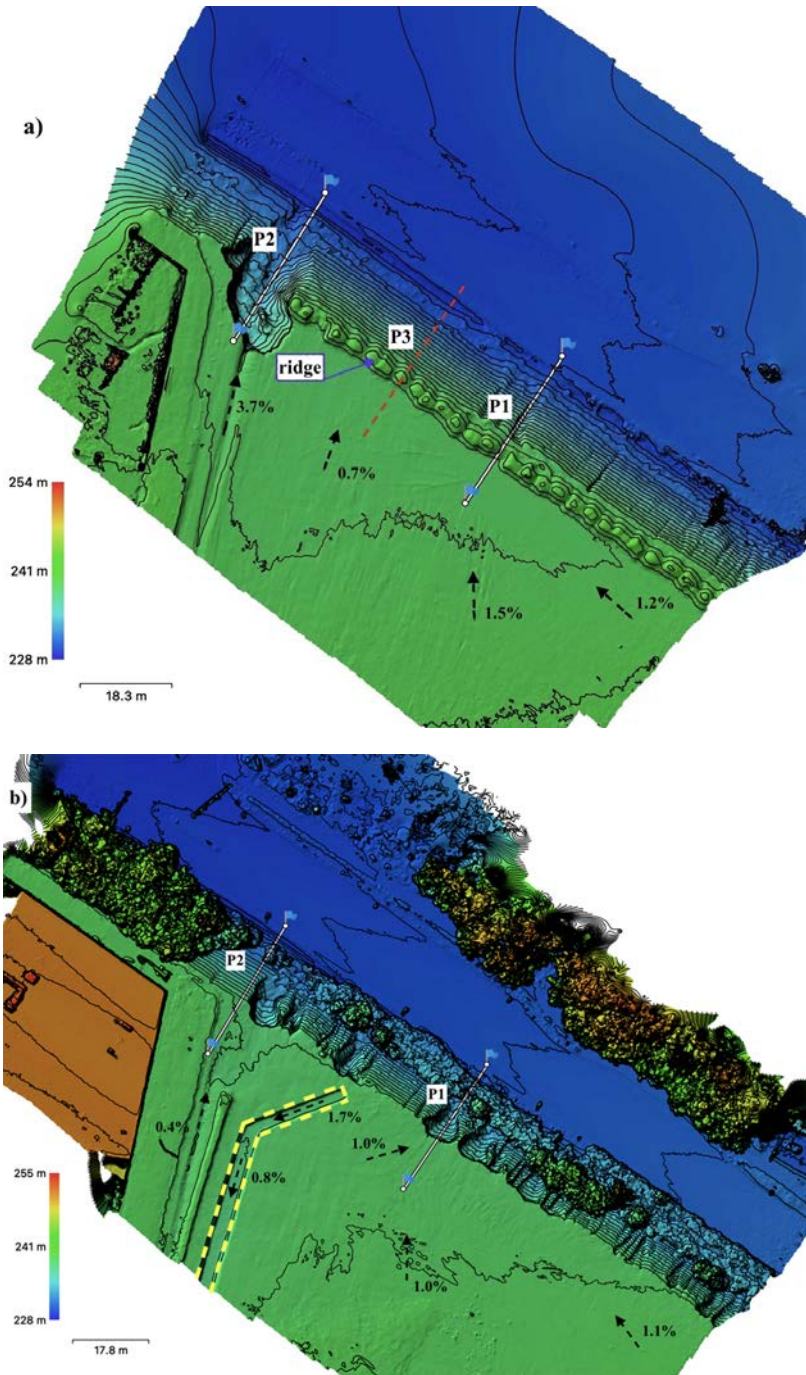


Fig. 3. DEM models with the cross-section lines and terrain slopes: a) 1st measurement (01.2022), b) 2nd measurement (06.2022)

every 0.5 meter of height. The main slopes of the upper surface of the dump (direction and % gradient) were assessed at several points (see the arrows in Fig. 3 and Fig. 4). To describe the observed failures, two cross-sections were chosen: P1 – with only slight disturbance in January 2022, and P2 – where the largest mass movement occurred on that day. The readings from January and June 2022 are compared in Fig. 4. A cross-section P3, representing the original undisturbed slope is shown there as well.

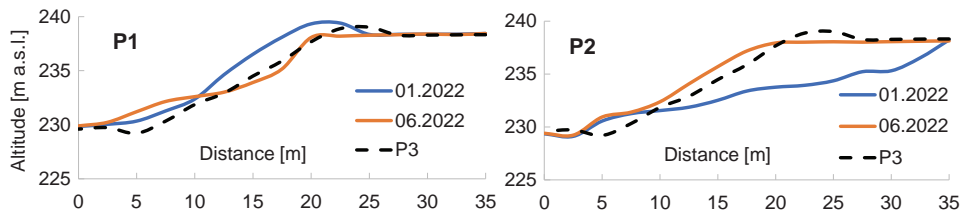


Fig. 4. Escarpment profiles: a) P1, b) P2

The original dump embankment (P3) was 8 m high with a slope 1:1.7, a ditch at the toe and a 1 m high ridge on the crown (compare with Fig. 3a). In the profile P1 in January 2022 only a minor mass movement was observed – a narrow gully was formed and some material from the upper part slid towards the ditch. The profile P2 from that day represents the effect of the slope failure at the zone of the largest observed depletion, reaching 11 meters into the embankment. The final shape of the damaged embankment suggests a compound type of slope failure: translational in the perpendicular cross-section and circular with almost vertical scarps in the longitudinal cross-section. Using the DEM, it was possible to calculate the volume of the lost material (the colluvium had been removed from the road pavement after the failure) – it was equal to about 1309.4 m³. It is worth noting that the main slopes of the upper surface of the dump, including the largest one (3.7%), were directed towards the place of the damage, which must have caused a constant inflow of water after the heavy rain to the analysed spot and was the most probable reason of the instability. After this failure, the void was filled with minestone, the escarpment was shaped to the original 1:1.7 slope and its surface was covered with the concrete slabs (see section P2 in Fig. 2). Additionally, a drainage canal was built (yellow dashed line in Fig. 3) with the inclination outwards the road. Unfortunately, these actions were not successful – in June 2022 the slope failures were not as deep as 6 months earlier, but they happened in several places (see also Fig. 2b). The forms of the failures were very similar to the largest one in January. As can be noticed from Fig. 3 the main slopes of the upper dump surface remained directed towards the road and between January and June 2022 the ridge was removed (the material was probably used for the refill) – it facilitated the access of rainwater to the escarpment.

To check whether the original 1:1.7 slope is safe in the considered case and to confirm whether the fluctuation of the water table is the main mechanism responsible for the repeating slope instabilities, slope stability analysis at the section P1 was conducted.

3.3. Numerical analysis of the slope stability

3.3.1. General remarks

The slope stability analysis can be conducted using one of the traditional ‘methods of slices’ (by Fellenius, Bishop, Janbu, etc.) or numerically, based on a finite difference or a finite elements method (FEM). The latter is the most often used in the difficult cases [26–29]. Contrary to the classical methods, FEM enables simulation of any ground conditions (including seepage flow or complicated geometry) and without any initial assumptions of the shape and location of the possible failure surface. It is also possible to simulate precisely the complete structure in three dimensions [30]. To conduct a reliable numerical analysis of the slope stability it is required to know the true current dimensions of the embankment (height and slope inclination) – here provided by the photogrammetric measurements using UAV, and to use appropriate, well calibrated constitutive models [31]. In the case of landfills in the close vicinity of roads the required minimum value of the factor of safety F_s (defined as the ratio of the generalized passive forces maintaining the system to the forces causing the failure) shall not be smaller than 1.3 [32].

3.3.2. Geotechnical properties

The slope stability check belongs to the few cases where the description of the (non-linear) soil stiffness is less important than the shear strength and where the simplest linear elastic-perfectly plastic Coulomb-Mohr model may be used without compromising the reliability of the results. Unfortunately, determination of the short list of the needed mechanical (effective cohesion c' and internal angle of friction φ' , undrained shear strength c_u , dilatancy angle ψ , elastic modulus E , Poisson ratio ν) and physical parameters (coefficient of permeability k , bulk density ρ) is not easy when the post-mining waste is concerned. Typical *in situ* tests (e.g. piezocone penetration CPTu, dilatometer test DMT, dynamic probing DP) cannot be applied due to the heterogeneity of the material, high content of very coarse fractions and lack of appropriate correlations. The choice of laboratory methods is even more limited – e.g. when shear strength parameters are concerned – the only option would be a large-scale direct shear box, but even the largest machine available on the world’s market with the box width of 1000 mm would not be able to accommodate grains larger than 60 mm in diameter. On the other hand, conducting the tests only on smaller fraction and applying some correction factors afterwards would be burdened with large error as the mineralogical composition, particle densities and porosity of the smaller and larger fractions are different [33]. It shall be noted that the material from the same coal level may have a different petrographic and mineral composition, which obviously influences the parameter values [34]. Moreover, the physical and mechanical properties of the fresh coal waste change after longer storage – due to weathering the content of finer fractions increases with time and the shear strength of the material drops. This process is most intensive in the external layers down to about 30–50 cm. In some coal mine dumps, especially the ones containing pyrite-rich minestone, a spontaneous combustion may occur, resulting in further change of the material properties [35]. All these factors make the coal waste an exceptionally difficult material. The values of the geotechnical parameters change in large

ranges and the results obtained from one landfill will not necessarily apply to some other even if the material seems to be macroscopically similar. The most reliable in terms of determination of the shear strength parameters would be probably the results of destructive trial *in situ* loading tests [36], while the best method to assess the value of the coefficient of permeability would be *in situ* pumping tests – such analyses are extremely rare.

Some values of the basic physical and mechanical parameters of unburnt (black) carbonaceous shales from Upper Silesia obtained in medium scale laboratory tests (at soil grading below 63 mm) reported in literature are presented in Table 1. The values sourced from B. Kawalec's thesis [33] refer to the unburnt dump shale from the KWK Gliwice mine (tested in oedometer ring 520 mm in diameter and shear box 480 mm in width), so are supposedly the most representative for the analysed case. It is assumed that the given shear strength parameters represent peak values in drained conditions. None of the published manuscripts reports the values of c_u , which are necessary in the undrained analyses of fine soils, even though the permeability coefficients of the material are not much different than the ones of silts or clayey silts as shown in Table 1. It shall be mentioned here that several embankment and coal mine dump failures occurred due to increase in pore water pressure and seepage pressure, resulting from rainfall infiltration [3, 27, 37]. The case considered in this paper seems to belong to one of them.

Table 1. Geotechnical parameters of unburnt carbonaceous shales deposited in dumps in Upper Silesia

Source	k , m/s	c , kPa	φ , °	E , MPa*	ρ , t/m ³
[33]	–	20–34	40–43	9.0 (25–49 kPa) 13.5 (49–98 kPa) 19.9 (98–196 kPa) 30.9 (196–392 kPa)	1.36–1.64
[25, 38]	10^{-4} – 10^{-7}	2–80	26–50	5.4 (0–50 kPa) 6.7–44.5 (50–300 kPa)	1.43–2.22 (old)
[39]	$7.4 \cdot 10^{-5}$ ($I_S = 0.90$) $1.4 \cdot 10^{-6}$ ($I_S = 0.97$) (at 10 kPa)	26.6	36.0	–	2.28

* Based on results of oedometric tests and Poisson's ratio $\nu = 0.2$

Eventually, in the numerical analysis the following values of the geotechnical parameters were assumed: $\varphi' = 36^\circ$, $c' = 5$ kPa, $E = 40$ MPa, $\nu = 0.20$, $k = 10 \cdot 10^{-6}$ m/s, $\rho = 1.9$ t/m³, $\rho_d = 1.69$ t/m³. The value of cohesion was taken as the minimum that was not causing calculation divergence at the shallow depths.

3.3.3. Numerical model

Z_Soil 2020 [40] FEM software was used to verify the stability of the slope. Plane strain state was assumed for the sake of simplification. The complex problems of water

infiltration and the resulting seepage pressure, together with the soil deformation caused by the change of effective stress were considered. The Terzaghi's theory with uncoupled consolidation was used, which means that the changes in the state of stress and strain did not influence the process of filtration (no hydro-mechanical coupling).

The initial dimensions of the numerical model represented the P1 section of the dump measured in January 2022. The model contained the scarp with the appropriate width of the crown and base – see Fig. 5, which ensured that the boundary conditions did not affect the obtained results. The depth of the analysed subsoil was chosen in a similar way. The correctness of the model dimensions was verified by confirming that a larger size of the model did not influence the location and shape of the failure surface. Four-node quadrangular finite elements were used to create the mesh. At each node, the searched unknowns were the two components of the displacement vector (in the horizontal and vertical directions) and the value of the pore water pressure. The standard geotechnical boundary conditions were applied: the displacements at the lower edge of the model were blocked in both perpendicular directions, together with the horizontal displacements at the side edges. The seepage through the base and the side edges of the model was made impossible. In the filtration analyses, the water table level at the base of the escarpment was fixed (left side in Fig. 5) at the bottom of the drain located at the toe. On the other side of the slope, several variants were considered with the groundwater table (GWT) at different depths below the top ground surface ($\Delta\text{GWT} = 2\text{--}10.5\text{ m}$). The steady state of flow was assumed. The other considered factor was the value of the distributed flux through the slope and the upper surface of the dump ('seepage' elements). It simulated various rainfall intensity.

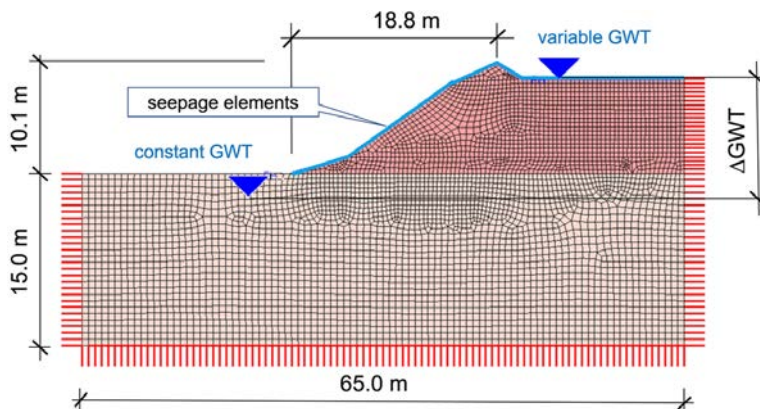


Fig. 5. Numerical FEM model of the analysed case

The numerical analyses included two stages. At the first one, the geostatic effective stress state and pore water pressure in the subsoil were calculated. The previous loading history (forming of the embankment) was not taken into account. At the second stage of the analysis, the slope stability was assessed. The 'c – tan φ reduction' method was applied to determine the factor of safety [28, 29]. The shape, location and extent of the slip surface,

corresponding to the obtained value of F_s , were identified from the map of displacements. It should be clearly noted here that the displacements at this stage of the analysis are virtual and can be used only for the assessment of the mechanism of the instability. It is not possible to assess the true values of displacements and compare them, for example, with the results of the geodetic measurement.

3.3.4. Results of the analysis

The results of the slope stability analysis at $\Delta\text{GWT} = 8$ m and rainfall intensity (RI) of 0.04 m/d are shown in Fig. 6. The obtained factor of safety is equal to $F_s = 1.42$. This means that at the favourable atmospheric conditions (just light rainfall) the slope remains stable, even if the water table difference is relatively high. The shape of the failure surface is similar to the one observed in the photogrammetric measurements in June 2022 (relatively shallow, not reaching below the toe of the escarpment).

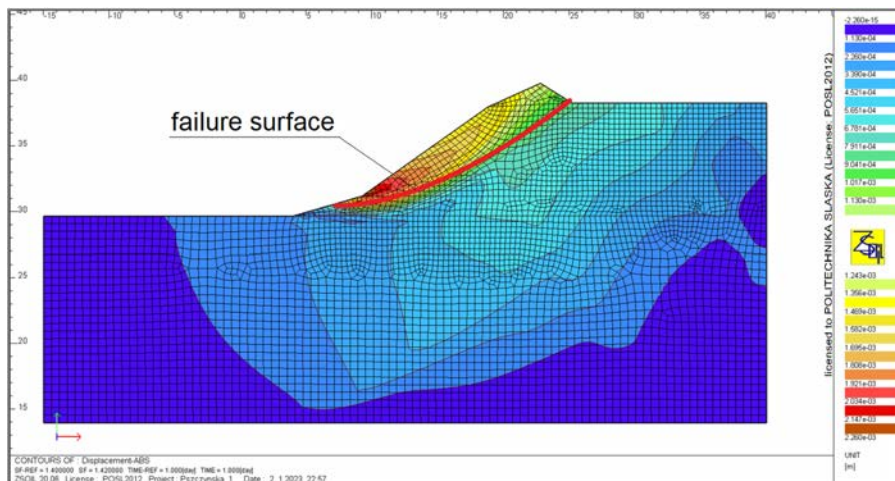


Fig. 6. Map of absolute displacements at the time of failure ($F_s = 1.42$)

The influence of the ground water table difference (head) between the two sides of the model and the infiltration rate caused by rainfall on the F_s value are presented in Fig. 7. It is clear that the both factors are strongly correlated with the decrease of safety. At medium rain (RI above 0.06 m/d) or if the water accumulation at the higher side of the escarpment is greater than 8 m (expected after long-lasting intensive precipitation) the risk of slope instability is becoming high ($F_s < 1.3$). In the assumed ground conditions, the rainfall intensity corresponding to heavy rain (RI above 0.18 m/d) means the inevitable occurrence of a landslide. As the observed failures occur practically after each heavy rain, these results confirm that the occurrence of water is the main factor responsible for the instabilities.

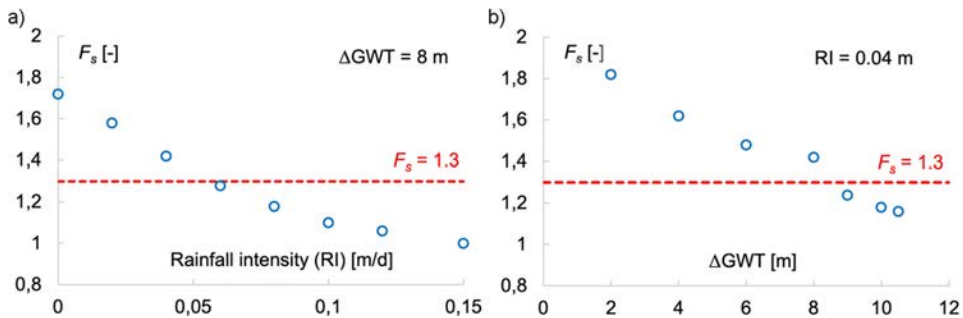


Fig. 7. Dependence of the factor of safety value on: a) rainfall intensity, b) water level difference

4. Summary and conclusions

Photogrammetric measurements conducted with the use of UAV allowed to determine the most important geometrical data of the analysed post-mining dump at Pszczyńska Street in Gliwice, without the necessity to enter into the unstable zone. The FEM numerical model, using the ‘ $c - \tan \varphi$ reduction’ method and parameter values assessed on the basis of literature review confirmed that the main factor initiating the repeatable slope failures in the dump escarpment is the rain water. The seepage pressure decreases the shear strength of the material by lowering the effective confining stress and eventually resulting in the safety factor $F_s < 1$ at even medium rainfall intensity. The flowing water is also obviously eroding the ground surface and flushing out the finest fractions (suffusion) which has an additional negative impact on the mechanical parameters of the material and on the slope stability. The 3D models, obtained from the post-processing of the digital images taken in two UAV missions with 6 months interval, revealed that the protective measures applied by the owner of the structure (covering the slope with concrete slabs and execution of one drainage canal in the vicinity of the industrial hall) were not successful. Removal of the ridge at the crown of the escarpment had also a detrimental effect on the slope safety. In the authors opinion, to prevent the future failures, the main slope of the upper surface of the dump along the whole length of the endangered road, should be inclined towards a new drainage canal constructed along the escarpment at large distance from it. A decrease of the embankment slope would be also helpful.

References

- [1] M. Łupieżowiec, J. Rybak, Z. Różański, P. Dobrzycki, and W. Jędrzejczyk, “Design and construction of foundations for industrial facilities in the areas of former post-mining waste dumps”, *Energies*, vol. 15, no. 16, art. no. 5766, 2022, doi: [10.3390/en15165766](https://doi.org/10.3390/en15165766).
- [2] G. Jordan and M. D’Alessandro, Eds., *Mining, mining waste and related environmental issues: problems and solutions in Central and Eastern European Candidate Countries*. European Communities, 2004.
- [3] A. Kainthola, D. Verma, S.S. Gupta, and T.N. Singh, “A coal mine dump stability analysis – a case study”, *Geomaterials*, vol. 1, no. 1, pp. 1–13, 2011, doi: [10.4236/gm.2011.11001](https://doi.org/10.4236/gm.2011.11001).

- [4] O. Igwe, C.N. Ayogu, R.I. Maduka, N.O. Ayogu, and T.A.S. Ugwoke, "Slope failures and safety index assessment of waste rock dumps in Nigeria's major mines", *Natural Hazards*, vol. 115, pp. 1331–1370, 2023, doi: [10.1007/s11069-022-05597-0](https://doi.org/10.1007/s11069-022-05597-0).
- [5] P.K. Behera, K. Sarkar, A.K. Singh, A.K. Verma, and T.N. Singh, "Dump slope stability analysis – A case study", *Journal of the Geological Society of India*, vol. 88, no. 6, pp. 725–735, 2016, doi: [10.1007/s12594-016-0540-4](https://doi.org/10.1007/s12594-016-0540-4).
- [6] K.S. Osasan and T.B. Afeni, "Review of surface mine slope monitoring techniques", *Journal of Mining Science*, vol. 46, no. 2, pp. 177–186, 2010, doi: [10.1007/s10913-010-0023-8](https://doi.org/10.1007/s10913-010-0023-8).
- [7] S. Artese and M. Perrelli, "Monitoring a landslide with high accuracy by total station: A DTM-based model to correct for the atmospheric effects", *Geosciences*, vol. 8, no. 2, 2018, doi: [10.3390/geosciences8020046](https://doi.org/10.3390/geosciences8020046).
- [8] M. Kulupa, P. Magda, and M. Mrówczyńska, "Accuracy characteristics of the selected diagnostics methods and the adjustment of geodetic observations", *Civil and Environmental Engineering Reports*, vol. 31, no. 4, pp. 167–183, 2021, doi: [10.2478/ceer-2021-0055](https://doi.org/10.2478/ceer-2021-0055).
- [9] O. Baykal, E. Tari, M. Z. Coşkun, and T. Erden, "Accuracy of point layout with polar coordinates", *Journal of Surveying Engineering*, vol. 131, no. 3, pp. 87–93, 2005, doi: [10.1061/\(ASCE\)0733-9453\(2005\)131:3\(87\)](https://doi.org/10.1061/(ASCE)0733-9453(2005)131:3(87)).
- [10] M. Wróblewska and M. Grygierek, "Assessment of visual representation methods of linear discontinuous deformation zones in the right-of-way", *Applied Sciences*, vol. 12, no. 5, art. no. 2538, 2022, doi: [10.3390/app12052538](https://doi.org/10.3390/app12052538).
- [11] B.X. Nam, T. Van Anh, L.K. Bui, N.Q. Long, T. Le Thu Ha, and R. Goyal, "Mining-Induced land subsidence detection by persistent scatterer InSAR and Sentinel-1: application to Phugiao Quarries, Vietnam", in *Proceedings of the International Conference on Innovations for Sustainable and Responsible Mining*, vol. 108, D. Tien Bui, H.T. Tran, and X.-N. Bui, Eds. Cham: Springer International Publishing, 2021, pp. 18–38, doi: [10.1007/978-3-030-60269-7_2](https://doi.org/10.1007/978-3-030-60269-7_2).
- [12] H. Ren, Y. Zhao, W. Xiao, and Z. Hu, "A review of UAV monitoring in mining areas: current status and future perspectives", *International Journal of Coal Science & Technology*, vol. 6, no. 3, pp. 320–333, 2019, doi: [10.1007/s40789-019-00264-5](https://doi.org/10.1007/s40789-019-00264-5).
- [13] U.S. Lay, B. Pradhan, Z.B.M. Yusoff, A.F.B. Abdallah, J. Aryal, and H.-J. Park, "Data mining and statistical approaches in debris-flow susceptibility modelling using Airborne LiDAR data", *Sensors*, vol. 19, no. 16, 2019, doi: [10.3390/s19163451](https://doi.org/10.3390/s19163451).
- [14] B. Kršák, et al., "Use of low-cost UAV photogrammetry to analyze the accuracy of a digital elevation model in a case study", *Measurement*, vol. 91, pp. 276–287, 2016, doi: [10.1016/j.measurement.2016.05.028](https://doi.org/10.1016/j.measurement.2016.05.028).
- [15] F. Elghaish, S. Matarneh, S. Talebi, M. Kagioglou, M. R. Hosseini, and S. Abrishami, "Toward digitalization in the construction industry with immersive and drones technologies: a critical literature review", *Smart and Sustainable Built Environment*, vol. 10, no. 3, pp. 345–363, 2021, doi: [10.1108/SASBE-06-2020-0077](https://doi.org/10.1108/SASBE-06-2020-0077).
- [16] K. Pawlak and D. Serek, "High voltage transmission line stringing operation. Usage of unmanned aerial vehicles for installation of conductor and grounding wires with optical fibers", in *2017 15th International Conference on Electrical Machines, Drives and Power Systems (ELMA)*. Sofia, Bulgaria, 2017, pp. 32–37, doi: [10.1109/ELMA.2017.7955396](https://doi.org/10.1109/ELMA.2017.7955396).
- [17] J. Howard, V. Murashov, and C.M. Branche, "Unmanned aerial vehicles in construction and worker safety", *American Journal of Industrial Medicine*, vol. 61, no. 1, pp. 3–10, 2018, doi: [10.1002/ajim.22782](https://doi.org/10.1002/ajim.22782).
- [18] M. Gheisari and B. Esmaili, "Unmanned Aerial Systems (UAS) for construction safety applications", in *Construction Research Congress 2016: Old and new construction technologies converge in historic San Juan*. ASCE: 2016, pp. 2642–2650, doi: [10.1061/9780784479827.263](https://doi.org/10.1061/9780784479827.263).
- [19] S. Zhou and M. Gheisari, "Unmanned aerial system applications in construction: a systematic review", *Construction Innovation*, vol. 18, no. 4, pp. 453–468, 2018, doi: [10.1108/CI-02-2018-0010](https://doi.org/10.1108/CI-02-2018-0010).
- [20] M.C. Tatum and J. Liu, "Unmanned aircraft system applications in construction", *Procedia Engineering*, vol. 196, pp. 167–175, 2017, doi: [10.1016/j.proeng.2017.07.187](https://doi.org/10.1016/j.proeng.2017.07.187).
- [21] C. Vanneschi, M. Eyre, M. Francioni, and J. Coggan, "The use of remote sensing techniques for monitoring and characterization of slope instability", *Procedia Engineering*, vol. 191, pp. 150–157, 2017, doi: [10.1016/j.proeng.2017.05.166](https://doi.org/10.1016/j.proeng.2017.05.166).

- [22] S. Coccia, M. Al Heib, and E. Klein, "Combination of UAV-borne LiDAR and UAV-borne photogrammetry to assess slope stability", presented at the The 7th World Congress on Civil, Structural, and Environmental Engineering, Apr. 2022, doi: [10.11159/icgre22.107](https://doi.org/10.11159/icgre22.107).
- [23] N. Ngadiman, I.A. Badrulhissham, M. Mohamad, N. Azhari, M. Kaamin, and N.B. Hamid, "Monitoring slope condition using UAV technology", *Civil Engineering and Architecture*, vol. 7, no. 6A, pp. 1–6, 2019, doi: [10.13189/cea.2019.071401](https://doi.org/10.13189/cea.2019.071401).
- [24] "Zniknie hałda z Puszczynskiej. Poszerzą się Nowe Gliwice?", *Nowiny Gliwickie*. [Online]. Available: <https://www.nowiny.gliwice.pl/zniknie-halda-z-puszczynskiej-poszerza-sie-nowe-gliwice>. [Accessed: 19 Dec. 2022].
- [25] K. M. Skarżyńska, "Reuse of coal mining wastes in civil engineering – Part 1: Properties of minestone", *Waste Management*, vol. 15, no. 1, pp. 3–42, 1995, doi: [10.1016/0956-053X\(95\)00004-J](https://doi.org/10.1016/0956-053X(95)00004-J).
- [26] A. Urbański and M. Grodecki, "Protection of a building against landslide. A case study and FEM simulations", *Bulletin of the Polish Academy of Sciences Technical Sciences*, vol. 67, no. 3, pp. 657–664, 2019, doi: [10.24425/BPASTS.2019.128545](https://doi.org/10.24425/BPASTS.2019.128545).
- [27] M. Jastrzębska and M. Łupieżowiec, "Analysis of the causes and effects of landslides in the Carpathian flysch in the area of Miłówka and evaluation of their prevention methods", *Annals of Warsaw University of Life Sciences – SGGW. Land Reclamation*, vol. 50, no. 2, pp. 195–211, 2018, doi: [10.2478/ssgw-2018-0016](https://doi.org/10.2478/ssgw-2018-0016).
- [28] Y. Zheng, X. Tang, S. Zhao, C. Deng, and W. Lei, "Strength reduction and step-loading finite element approaches in geotechnical engineering", *Journal of Rock Mechanics and Geotechnical Engineering*, vol. 1, no. 1, pp. 21–30, 2009, doi: [10.3724/SP.J.1235.2009.00021](https://doi.org/10.3724/SP.J.1235.2009.00021).
- [29] J. Ślusarek and M. Łupieżowiec, "Analysis of the influence of soil moisture on the stability of a building based on a slope", *Engineering Failure Analysis*, vol. 113, art. no. 104534, 2020, doi: [10.1016/j.engfailanal.2020.104534](https://doi.org/10.1016/j.engfailanal.2020.104534).
- [30] M. Cała, M. Kowalski, and A. Stopkiewicz, "The three-dimensional (3D) numerical stability analysis of Hyttmalmen Open-Pit", *Archives of Mining Sciences*, vol. 59, no. 3, pp. 609–620, 2014, doi: [10.2478/amsc-2014-0043](https://doi.org/10.2478/amsc-2014-0043).
- [31] M. Kowalska, "Influence of loading history and boundary conditions on parameters of soil constitutive models", *Studia Geotechnica et Mechanica*, vol. 34, no. 1, pp. 15–33, 2012, doi: [10.1515/sgem-2017-0020](https://doi.org/10.1515/sgem-2017-0020).
- [32] L. Wysokiński, *Ocena stateczności skarp i zboczy. Zasady wyboru zabezpieczeń – instrukcja*. Warszawa: ITB Publishing House, 2011.
- [33] B. Kawalec, "Właściwości fizyczne i mechaniczne odpadów kopalnianych jako gruntu budowlanego", PhD thesis, Politechnika Śląska, Gliwice, 1973.
- [34] J. Adamczyk, "Basic geotechnical properties of mining and processing waste – a state of the art analysis", *AGH Journal of Mining and Geoengineering*, vol. 36, no. 2, pp. 31–41, 2012.
- [35] M. Onifade and B. Genc, "Spontaneous combustion of coals and coal-shales", *International Journal of Mining Science and Technology*, vol. 28, no. 6, pp. 933–940, 2018, doi: [10.1016/j.ijmst.2018.05.013](https://doi.org/10.1016/j.ijmst.2018.05.013).
- [36] J. Kawalec, "In situ tests as the method of strength parameters determination for mining waste", presented at the International Conference on In Situ Measurement of Soil Properties and Case Histories, Bali, Indonesia, May 2001.
- [37] J. Kim, S. Jeong, S. Park, and J. Sharma, "Influence of rainfall-induced wetting on the stability of slopes in weathered soils", *Engineering Geology*, vol. 75, no. 3–4, pp. 251–262, 2004, doi: [10.1016/j.enggeo.2004.06.017](https://doi.org/10.1016/j.enggeo.2004.06.017).
- [38] K. M. Skarżyńska, *Odpady powęglowe i ich zastosowanie w inżynierii lądowej i wodnej*. Kraków: Akademia Rolnicza im. H. Kołłątaja, 1998.
- [39] T. Zydroń, A. Gruchot, and E. Zawisza, "Geotechnical characteristics of unburnt colliery spoils after coal-recovery", *MATEC Web Conferences*, vol. 262, art. no. 04006, 2019, doi: [10.1051/matec-conf/201926204006](https://doi.org/10.1051/matec-conf/201926204006).
- [40] S. Commend, S. Kivell, R. Obrzud, K. Podleś, and A. Truty, *Computational Geomechanics & Applications with ZSOIL.PC*. Lausanne: Zace Services Ltd, Software Engineering, 2020.

Analiza stateczności skarp hałd pokopalnianych z wykorzystaniem pomiarów fotogrametrycznych – studium przypadku

Słowa kluczowe: bezzałogowy statek powietrzny, ciśnienie sphywowe, fotogrametria, hałda pokopalniana, stateczność skarpy

Streszczenie:

Hałdy pokopalniane nadal stanowią typowy element w krajobrazie Górnego Śląska. Wiele z nich nie jest już użytkowana przez kopalnie węgla kamiennego jako miejsce składowania odpadów; została poddana procesom rekultywacji i przeznaczona na tereny inwestycyjne. Na takim obszarze mieści się np. katowicki „Spodek” czy Wojewódzki Park Kultury i Wypoczynku w Chorzowie. Często tereny te nie są jednak właściwie zabezpieczone i mimo rewitalizacji, niektóre nasypy mogą stanowić zagrożenie dla mieszkańców i środowiska. Przykładem takiego problemu jest hałda przy ulicy Pszczyńskiej w Gliwicach, będąca pozostałością po kopalni węgla kamiennego, która zakończyła wydobywanie w tym rejonie ponad 20 lat temu. Na długości ok. 600 metrów skarpa o wysokości ok. 8 m sąsiaduje bezpośrednio z ruchliwą drogą. Wielokrotnie, zwykle po ulewnych opadach deszczu, następowały na tym obszarze osuwiska skutkujące zamknięciem znacznego odcinka drogi dla ruchu kołowego. Tego typu miejsca wymagają stałej obserwacji geodezyjnej i kontroli stateczności. W wielu przypadkach trudno jest ustalić właściciela hałdy, przez co wejście w teren w celu wykonania klasycznych pomiarów geodezyjnych jest utrudnione. Dodatkowo z uwagi na często strome i wysokie skarpy, wykonywanie pomiarów klasycznych może stanowić zagrożenie dla osób mierzących. Wówczas przydatne stają się techniki zdalne, takie jak wykorzystanie bezzałogowego statku powietrznego (BSP, potocznie: „dron”). Wyniki pomiarów mogą być następnie wykorzystane w analizach numerycznych dotyczących stateczności skarp. Problematiczne oczywiście pozostaje ustalenie wartości parametrów modeli konstytutywnych reprezentujących materiał budujący hałdę.

W niniejszym artykule na przykładzie hałdy zlokalizowanej na terenie miasta Gliwice pokazano możliwości, jakie daje wykorzystanie fotogrametrii oraz bezzałogowych statków powietrznych (BSP) do cyklicznych kontroli stanu nasypów. Obserwowano aktualny stan zwałowiska oraz efekty naprawy po dwóch przypadkach awarii skarpy. Podczas dwóch misji lotniczych wyznaczono główne spadki powierzchni terenu oraz wybrane przekroje poprzeczne. Uzyskane dane geometryczne wykorzystano w dalszej analizie numerycznej. Zdefiniowano model z wykorzystaniem Metody Elementów Skończonych, reprezentujący jeden z przekrojów skarpy w celu oszacowania współczynnika bezpieczeństwa oraz określenia głównych mechanizmów odpowiedzialnych za awarię. Do opisu zachowania ośrodka gruntowego wykorzystano sprężysto-idealnie plastyczny model Coulomba-Mohra, a w analizie stateczności użyto metody redukcji wytrzymałości „ $c - \tan \varphi$ ”. Zwrócono uwagę na problem wiarygodnego oszacowania właściwości materiałów. W analizie uwzględniono wpływ ciśnienia sphywowego i różnicy naporów na stateczność skarpy. Stwierdzono, że decydujący wpływ na niestabilność zwałowiska miała intensywność opadów deszczu.

Received: 2023-03-31, Revised: 2023-04-11